

Volume and Potential Vorticity Budgets of Eighteen Degree Water

BRUNO DEREMBLE AND W. K. DEWAR

Department of Earth, Ocean and Atmospheric Science, The Florida State University, Tallahassee, Florida

(Manuscript received 14 March 2013, in final form 17 July 2013)

ABSTRACT

Mode waters are a distinctive baroclinic feature of the World Ocean characterized by relatively weak vertical stratification. They correspond dynamically to low potential vorticity (PV). In the North Atlantic subtropical gyre, the mode waters have become known as Eighteen Degree Water. Their dynamics involves air–sea interaction, diapycnal and isopycnal mixing, and subduction. Understanding mode water dynamics is therefore both challenging and important since it connects several aspects of the ocean circulation. Mass and PV budget of the mode water’s core, evaluated in a realistic primitive equation North Atlantic model, are used to characterize mode water maintenance. It is shown that the surface PV flux has very little impact on mode water; the surface buoyancy flux in combination with eddy mass flux is the most important control on mode water structure. A mean PV formalism is used to show that the PV and water-mass formation budgets are intrinsically linked. A decomposition of the budget demonstrates the role of the mean PV field in permitting the eddy mass flux to discharge the net formation to the surrounding fluid.

1. Introduction

Mode water, characterized as a pool of weakly stratified temperature and salinity, and hence density, is found in the equatorial flank of all major western boundary currents (Hanawa and Talley 2001). The subtropical North Atlantic mode water is a layer 200–300 m thick and 300 m deep located south of the Gulf Stream, characterized by a temperature of 18°C and a salinity of 36.4 psu. The persistence of these properties, particularly the temperature, has motivated their nickname of Eighteen Degree Water (EDW). Another way to identify mode waters is to use potential vorticity (PV). The large-scale PV is

$$Q_{ls} = -\frac{f}{\rho_0} \sigma_z, \quad (1)$$

with f the planetary vorticity, ρ_0 a reference density, σ the potential density, and $\sigma_z = \partial\sigma/\partial z$ (notation used henceforth) the vertical density gradient. According to this definition, the weak stratification of mode waters

maps into low PV values. Regions of minimum PV values are now routinely identified as mode waters, an association that hints at a unique dynamical character.

Historically, mode waters were among the first water masses to be well documented. An early observation of EDW is found in the 1873 *Challenger* data. Its persistence to modern times clearly identifies EDW as a feature of the mean stratification. Worthington (1958) examined North Atlantic mode waters and proposed their now traditional name “Eighteen Degree Water.” He also suggested that late wintertime cold air outbreaks over the Gulf Stream were the primary reason that EDW is found where it is. Warren (1972) in a following study suggested local convection was a weak source of mode water, arguing that the primary role of the strong regional heat fluxes just south of the Gulf Stream was to eat away the seasonal thermocline above EDW rather than to generate much new volume in the EDW temperature range.

There are only a few dynamical theories that purport to explain the existence of mode waters. Perhaps the first is Dewar (1986), who extended the homogenization ideas of Rhines and Young (1982) to include diabatic effects. Marshall (2000) predicted the existence of a low PV layer using an integral constraint on PV. A competing theory is Dewar et al. (2005), who applied ventilated thermocline mechanics to the problem. In the

Corresponding author address: Bruno Deremble, The Florida State University, 117 N. Woodward Ave., Tallahassee, FL 32306-4320.

E-mail: bderemble@fsu.edu

latter, the thick layer of mode water was explained as the result of Ekman pumping operating inside the western recirculation zone predicted by ventilated thermocline theory. The pumping in such a zone was envisioned as proceeding in the absence of any competing mass fluxes, thus squeezing the subsurface layer away. The compensating thickened surface layer was then identified as mode water. This theory neglected eddy dynamics, as is characteristic of the ventilated thermocline framework.

Our analysis here will bear more in common with Dewar (1986), so we review it in a bit more detail. In a quasigeostrophic framework, the mean PV equation for a subsurface layer not exposed to wind stress is

$$J(\bar{\psi}, \bar{q}) = -\nabla \cdot (\bar{\mathbf{u}}'q') + D, \quad (2)$$

where ψ is the geostrophic streamfunction, D is a parameterized diabatic flux driven by surface heat loss, \mathbf{u} is the geostrophic velocity, q is the quasigeostrophic PV, where

$$q = \nabla^2 \psi + \beta y - \frac{f_o h}{H}, \quad \text{and} \quad (3)$$

the overbar implies a time average. In the above, f_o is the Coriolis parameter, J the usual Jacobian, β the beta parameter, H a resting state fluid layer thickness, and h is a layer thickness anomaly relative to H . Equation (2) equates mean PV flux divergence to eddy flux divergence and diabatic forcing. We expect for regions of heat loss, like the area just south of the Gulf Stream, that D will reduce PV and hence is negative. Assuming a closed circulation contour ($\bar{q} = \bar{q}_o$) that bounds a domain Ω and integrating over Ω yields the exact result

$$0 = -\int_{\partial\Omega} \bar{\mathbf{u}}'q' \cdot \mathbf{n} \, dl + \iint_{\Omega} D \, dA. \quad (4)$$

In Eq. (4), \mathbf{n} is the outward normal vector on the bounding contour $\partial\Omega$.

If the standard homogenization assumption is made that eddies flux PV down the mean gradient with a diffusivity coefficient κ , Eq. (4) can be written

$$-\kappa \int_{\partial\Omega} \nabla \bar{q} \cdot \mathbf{n} \, dl = \iint_{\Omega} D \, dA. \quad (5)$$

Employing the solution of Eq. (2) $\bar{q} = \bar{q}(\bar{\psi})$ that applies if diabatics and eddy fluxes are "weak," Eq. (4) becomes

$$\left. \frac{d\bar{q}}{d\bar{\psi}} \right|_{q_0} = -\frac{\iint_{\Omega} D \, dA}{\int \kappa \nabla \bar{\psi} \cdot \mathbf{n} \, dl}. \quad (6)$$

Note that in the absence of diabatic effects ($D = 0$ inside Ω), Eq. (6) predicts uniform PV. For net cooling in an anticyclone, Eq. (6) predicts the generation of a low PV, with the production of low PV by heat loss balanced against the influx of high PV from the outside driven by the eddies. This theory emphasizes eddy mechanics as central to mode water maintenance, and in this sense contrasts sharply with Dewar et al. (2005).

Potential vorticity in the primitive equations was examined in Haynes and McIntyre (1987), who showed that PV was governed by

$$\frac{\partial \rho_0 Q}{\partial t} + \nabla \cdot \mathbf{J} = 0, \quad (7)$$

where Q is Ertel PV

$$\rho_0 Q = -(\nabla \times \mathbf{u} + \mathbf{f}) \cdot \nabla \sigma \quad (8)$$

and \mathbf{J} was a generalized PV flux containing both advective and nonadvective parts. Further, \mathbf{J} was shown to not cross surfaces of constant potential density σ , leading to the now well-known impermeability theorem. Because of this, the PV of an isopycnal layer can be modified only at its outcrop at the surface or incrops on topography. Given the unique and clear PV signature of mode waters, the working hypothesis of many recent studies (Thomas 2005; Czaja and Hausmann 2009; Maze and Marshall 2011; Deremble and Dewar 2012; Olsina et al. 2013; Maze et al. 2013) has been that the surface sources of PV on those isopycnals would be distinctive in a way that explained the existence of mode waters. The role of the different processes affecting PV production (or destruction) is still a matter of debate (The Climode Group 2009; D'Asaro et al. 2011), although the above studies frequently concluded buoyant production of PV was the dominant surface source for the mode water densities.

Mode water formation can also be studied using the Walin formalism (Walin 1982). This approach combines the conservations of heat and salt and the conservation of mass to compute net water-mass formation. In this computation, the buoyancy fluxes at the surface due to heat and freshwater fluxes predict the formation or destruction of water in a given density class. This estimate is accurate provided that interior diapycnal mixing can be neglected (Nurser et al. 1999; Marshall et al. 1999). Speer and Tziperman (1992) were the first to use climatological data to compute water-mass formation. Since their study, there have been several attempts to quantify the mode water formation rate in the Atlantic. Until now, the value of this formation rate has remained uncertain. Forget et al. (2011) showed that, depending

on the formulation of the air–sea heat flux, the Walin estimate can vary from 2 to 12 Sv ($\text{Sv} \equiv 10^6 \text{ m}^3 \text{ s}^{-1}$) (see their Fig. 11). Maze et al. (2009) also computed errors on the formation rates. Studies using observational data to compute the Walin budget have traditionally worked in a domain bounded by lateral boundaries where no-flux conditions could be exploited in place of detailed subsurface observations.

The Walin analyses demonstrated skill in identifying mode water density ranges, but differed importantly from the surface PV flux studies in that it was rooted more in a water-mass framework than in a dynamical one. The question that we now ask is which of these processes (PV surface fluxes or water-mass formation) is responsible for the creation of mode water? Are the processes linked? If so, how do they combine?

To address these questions, we develop a formalism that relates the two approaches. We compute the two budgets for the mode water pool, PV, and mass, and establish that these budgets are linked using the PV formalism developed in a companion paper [Deremble et al. (2013), D13 hereafter]. We dissect the PV budget to extract its components, namely surface fluxes and interior fluxes. The interior fluxes are further decomposed into a mean and an eddy contribution. Since we are mostly interested in the mode water formation process, we compare the importance of PV fluxes and water-mass formation to the maintenance of the mode water core.

Numerical evaluation of these budgets is performed using an output from an ocean general circulation model (OGCM). We use the last 10 years of the NATL12 run (Treguier 2008), a $1/12^\circ$ run that, by modern standards, well resolves midlatitude ocean mesoscale activity (Treguier et al. 2012). Furthermore Maze et al. (2013) showed that the mode water in this model occurred on the observed density surfaces and had realistic temperature, salinity, and spatial distribution.

The paper is organized as follows. We introduce several definitions in section 2 and describe the modeled mode water. As opposed to observational studies, we can study domains smaller than the basin, so we also define the boundaries of the volume on which we apply the budgets. We describe and apply the Walin formalism in section 3, and formulate and apply the PV budget in section 4. Results from the Walin formation rate and PV budget are discussed in each section respectively. We separate the contributions from the mean flow and the eddies in the PV budget and quantify each of them in section 5. We also describe in this section how the Walin and PV budget are related. An extension of the mode water theory from a quasigeostrophic framework to a primitive equation setting is presented in section 6 and conclusions are given in section 7.

2. Definition of the control volume

In this section, we introduce the definition of thickness-weighted time averaging used hereafter. Thickness weighting has proved its utility in the parameterization of eddies for coarse-resolution models (Gent and McWilliams 1990; Treguier et al. 1997), and we use it here to define climatological-mean mode water.

a. Thickness-weighted time averaging

The classical Reynolds decomposition of a variable u is at any time

$$u(\mathbf{x}, t) = \bar{u}(\mathbf{x}) + u'(\mathbf{x}, t), \quad (9)$$

where \bar{u} denotes the time average of u and u' denotes the fluctuating part with zero mean; \mathbf{x} is the traditional three-dimensional position vector, and t the time. Thickness-weighted time averaging is defined as

$$\hat{u} = \frac{\bar{z}_\sigma \bar{u}}{\bar{z}_\sigma}, \quad (10)$$

with $z_\sigma = \partial z / \partial \sigma$, a measure of the vertical stratification; z is the height of the isopycnal σ . Henceforth, we use the subscript as a notation for the derivative with respect to a variable. The fluctuating part with respect to the mean \hat{u} is written u'' so that at any time

$$u(\mathbf{x}, t) = \hat{u}(\mathbf{x}) + u''(\mathbf{x}, t), \quad (11)$$

where u'' has a vanishing thickness-weighted mean. Note that the bolus velocity is $u^* = \hat{u} - \bar{u}$. In a continuously stratified model, there are several ways to compute the thickness-weighted time averaging. Henceforth, we will only be working with isopycnal layer of thickness $\Delta\sigma = \sigma_2 - \sigma_1$ (as opposed to isopycnal surface with zero thickness). Using a linear interpolation, one can find the heights z_1 and z_2 at which the density is equal to σ_1 and σ_2 (in the model output we are using, σ is always monotonically increasing from bottom to top). We compute z_σ using the discrete formulation: $z_\sigma = (z_2 - z_1) / (\sigma_2 - \sigma_1)$. When the isopycnal layer outcrops, the upper density σ_1 is replaced by the surface density and z_1 is set to zero. The value of u in the density layer is simply taken as the average of u between z_1 and z_2 using linear interpolation to find the value of u at z_1 and z_2 .

The climatological distribution of the model mode water is defined in terms of PV thickness-weighted time averaging. Recall the definition of PV is

$$Q = -\frac{1}{\rho_0} \boldsymbol{\omega} \cdot \nabla \sigma, \quad (12)$$

with $\boldsymbol{\omega}$ being the total vorticity: $\boldsymbol{\omega} = f \mathbf{k} + \nabla \times \mathbf{u}$. Given the $1/12^\circ$ resolution of the model, PV is represented very

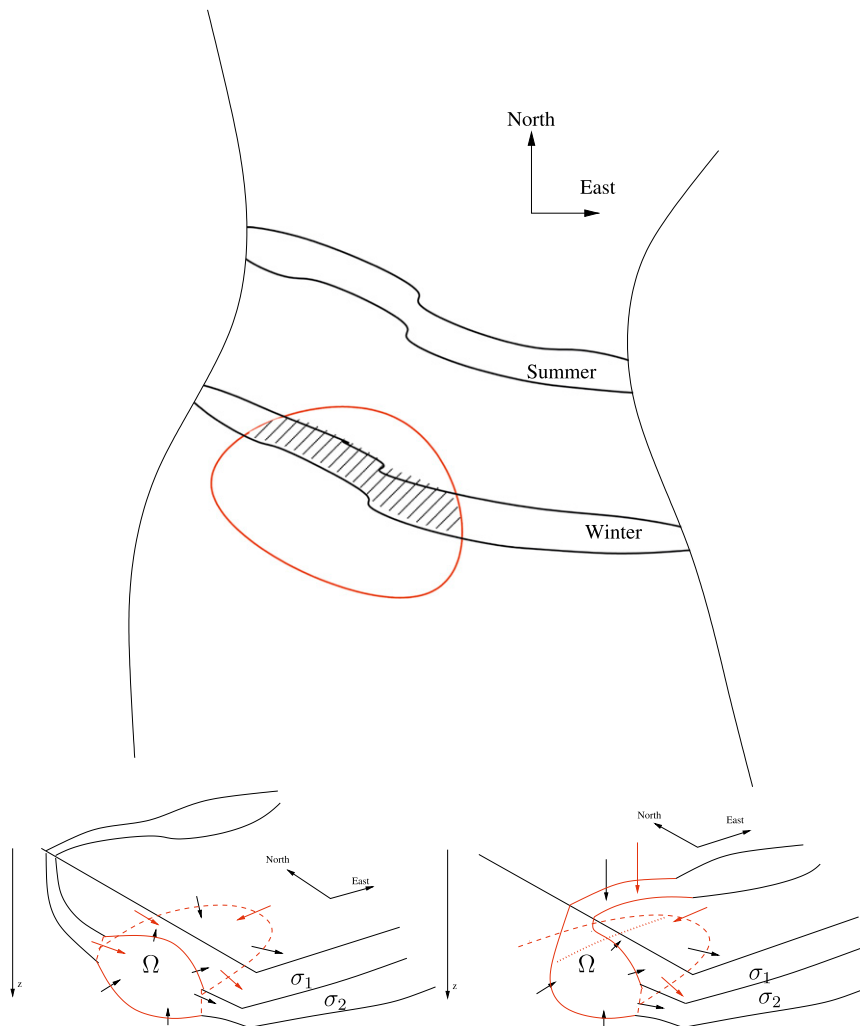


FIG. 1. Schematic of the control volume Ω : (top) top view. Contour \mathcal{C} is plotted in red. Also plotted are the positions of the summer and winter outcrop windows. The hatched area corresponds to a time when Ω is in contact with the atmosphere. (bottom) Side view of Ω encapsulated between two isopycnal surfaces. Black arrows represent the mass flux; red arrows are the PV flux. An idealized view of (left) summertime when the outcrop is outside \mathcal{C} and (right) wintertime with an outcrop inside \mathcal{C} .

accurately by its vertical component, an approximation we will adopt throughout this paper:

$$Q = -\frac{1}{\rho_0} (f + \mathbf{k} \cdot \nabla \times \mathbf{u}) \cdot \sigma_z. \quad (13)$$

The thickness-weighted time averaging of Q is then

$$\hat{Q} = -\frac{1}{\rho_0} \frac{\overline{f + \mathbf{k} \cdot \nabla \times \mathbf{u}}}{\overline{z_\sigma}}. \quad (14)$$

A practical result is that generally the Coriolis parameter dominates over relative vorticity, thus reducing the above \hat{Q} to the PV definition appearing in

Eq. (1). A property of thickness-weighted time averaging is

$$\overline{z_\sigma Q u} = \overline{z_\sigma} \hat{Q} \hat{u} + \overline{z_\sigma u'' Q''}, \quad (15)$$

an identity that is used in section 5 for the mean/eddy decomposition [see Peterson and Greatbatch (2001), for the use of this identity].

b. Definition of the boundaries

We now define a time-varying control volume Ω with boundaries $\partial\Omega$ inside of which we will compute various budgets. This volume, shown schematically by the red line in Fig. 1, is bounded above and below by isopycnals

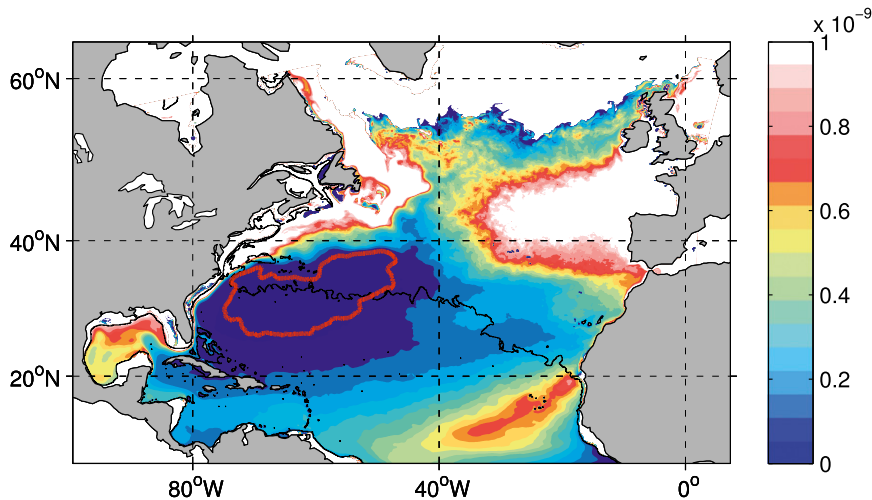


FIG. 2. Ten-year-mean thickness-weighted PV \hat{Q} on isopycnal 26.25. The red line corresponds to $\hat{Q} = 10^{-10} \text{ m}^{-1} \text{ s}^{-1}$. The black line (crossing this contour) is the southernmost position of the isopycnal 26.25 during these 10 years.

σ_1 and σ_2 , and at its largest extent laterally by a fixed, closed latitude, longitude curve. In general, the isopycnals σ_1 and σ_2 will outcrop inside the red curve, as indicated by the shading in Fig. 1. In this case, we will define our working volume as that volume closed to the north by the outcrops but everywhere else bounded by the red curve and the isopycnals. We expect that, as a result primarily of the seasonal cycle, periods will occur when the outcrops have migrated north of the red curve, in which case we define our working volume by the red curve and the bounding isopycnals.

Henceforth, we name the various components of $\partial\Omega$ as follows. The upper and lower density surfaces are labeled Σ_{σ_1} and Σ_{σ_2} , the side Σ_S , and the outcrop Σ_o .

We are interested in computing the mass and PV flux across $\partial\Omega$. In Fig. 1, these fluxes are depicted using black and red arrows, respectively. Mass flux is expected on all points of $\partial\Omega$, whereas no PV flux is expected across isopycnals because of the impermeability theorem (this point is further developed in section 4).

For all the numerical applications, we choose $\sigma_1 = \rho_0 + 26.15 \text{ kg m}^{-3}$ and $\sigma_2 = \rho_0 + 26.35 \text{ kg m}^{-3}$, with ρ_0 a reference density set to 1000 kg m^{-3} . For definiteness, we will later choose the red curve to coincide in space with the location of the climatological PV contour $\hat{Q} = 10^{-10} \text{ m}^{-1} \text{ s}^{-1}$ on the isopycnal surface 26.25 kg m^{-3} (henceforth, we omit the unit when labeling an isopycnal). We stress, however, that the following analysis is independent of these choices and applies to any \hat{Q} contour or any isopycnal range.

Figure 2 shows \hat{Q} on the isopycnal 26.25. Mode water is located in the low PV area (blue region inside the red contour). The boundary of our domain is chosen to coincide

with the innermost contour—a region for which \hat{Q} is lower than $10^{-10} \text{ m}^{-1} \text{ s}^{-1}$. Henceforth, we call this contour \mathcal{C} .

This contour is similar to the one selected by Maze et al. (2013), who used a temperature criterion (see their Fig. 1). The southernmost position of the isopycnal 26.25 outcrop is plotted with a black line in Fig. 2. It intersects the contour, meaning that during part of the year the northern boundaries of Ω will be in contact with the surface.

3. Volume budget

Having defined the boundaries of Ω , we now compute a mass budget. This mass, or equivalently in the present Boussinesq framework volume, budget is related to the surface buoyancy flux via the Walin formalism.

a. Mean mass budget

Marshall et al. (1999) discussed the Walin analysis for water-mass formation. We recap their demonstration here. The starting point is the continuity equation,

$$\nabla \cdot \mathbf{u} = 0, \quad (16)$$

and the equation of evolution of density,

$$\frac{\partial \sigma}{\partial t} + \nabla \cdot \mathbf{u} \sigma = -\nabla \cdot \mathbf{N}^\sigma + E, \quad (17)$$

where \mathbf{N}^σ represents nonadvective flux of density and E is the thermobaric contribution that cannot be cast in the gradient term. These two equations are integrated over the control volume Ω . They are then combined to obtain an estimate of the volume flux through the sides of the control volume,

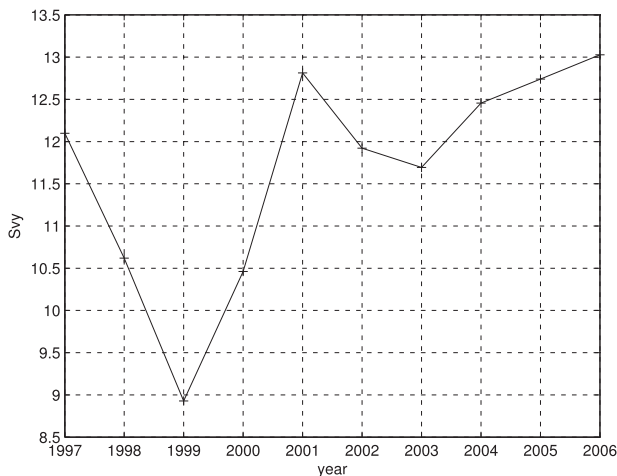


FIG. 3. Ten-year time series of the volume of water enclosed in the control volume Ω . Ordinate is Svy.

$$\int_{\Sigma_s} \sigma \mathbf{u} \cdot \mathbf{n} dA = \overline{F(\sigma_2)} - \overline{F(\sigma_1)}, \quad (18)$$

in which \mathbf{n} is the outward-pointing unit vector normal to Σ_s , and

$$F = \frac{\partial}{\partial \sigma} \int_{\Sigma_o(t)} \frac{\alpha}{c_p} Q_{\text{net}} dA \quad (19)$$

is the transformation rate (and where it has been assumed that interior diabatic fluxes and effects due to thermobaricity are negligible). In the previous equation, α is the thermal expansion coefficient, c_p is the heat capacity of seawater, and Q_{net} the air–sea heat flux. In our study, we neglect the component of the transformation rate owing to evaporation and precipitation and only consider the component due to the air–sea heat flux.

The Walin analysis suggests that the flux out of the control volume is dominated by the net formation at the surface. The most questionable assumption made here is the neglect of diapycnal diffusive fluxes. We will test this approximation later.

b. Evaluation in the model

The 10-yr time series of the annual mean of the volume inside Ω is shown in Fig. 3. The mean corresponding volume during this 10-yr period is 11.5 Svy (1 Svy \equiv 1 Sv \times 1 yr)—meaning that a sustained flux of 11.5 Sv during 1 year will entirely renew the water inside Ω . Of course, this number may vary depending on the definition of mode water (criteria for \hat{Q} and choice of σ_1 and σ_2). The standard deviation of the 10 points is 1.5 Svy. We also find the long-term volume trend to be $[V(10) - V(0)]/10\text{yr} = 0.1\text{ Sv}$. We will ignore such contributions in what follows.

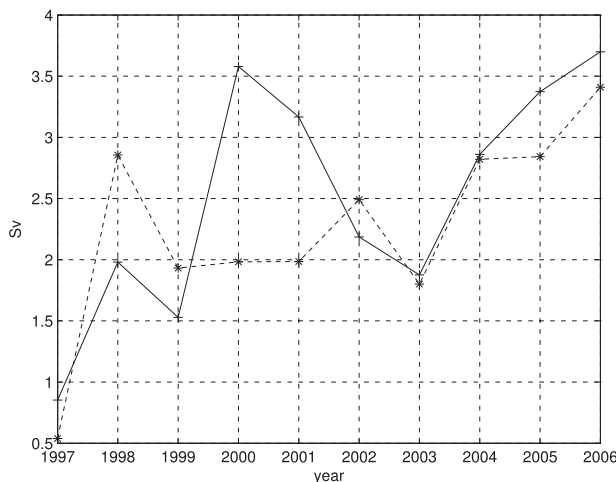


FIG. 4. Ten-year time series of the volume side flux (dashed line) [lhs of Eq. (18)] and the formation rate due to surface forcing (solid line) [rhs of Eq. (18)]. Ordinate is Sv. The mean of both time series is 2.5 Sv.

c. Validation of the Walin budget

To examine the Walin budget described in the previous section, we first evaluate Eq. (18) using successive 1-yr means. The 10-yr time series is plotted in Fig. 4—the dashed curve is the mean mass exiting Ω [lhs of Eq. (18)] and the solid line is the formation rate associated with the heat surface forcing [rhs of Eq. (18)]. The Walin formation rate is computed by evaluating $F(\sigma_1)$ and $F(\sigma_2)$ from Eq. (19) using the integral of the heat flux over an outcropping window of width $\Delta\sigma = 0.1$. The difference between $F(\sigma_2)$ and $F(\sigma_1)$ gives the formation rate. Freshwater forcing has not been taken into account to compute the buoyancy budget. The two curves are comparable (correlation coefficient: 0.9). According to this plot, there is a mean production rate of $2.5 \pm 0.9\text{ Sv}$ by surface forcing and a mean destruction by interior fluxes of $2.3 \pm 0.8\text{ Sv}$. The error bar corresponds to the standard deviation of the 10 points of each time series and reflects the interannual variability.

To take into account the variable volume of Ω (the storage), we plot in Fig. 5 the year-to-year average of the variation of the volume contained in Ω and the year-to-year average of the surface formation rate plus the exit side flux. This figure shows agreement between the variation of the volume and the out- and inward mass fluxes (correlation coefficient: 0.9).

4. Potential vorticity budget

As mentioned earlier, mode water is characterized by its low PV. A PV budget on the control volume Ω is thus necessary to quantify entry flux and exit flux of PV, and more generally the pathway of PV.

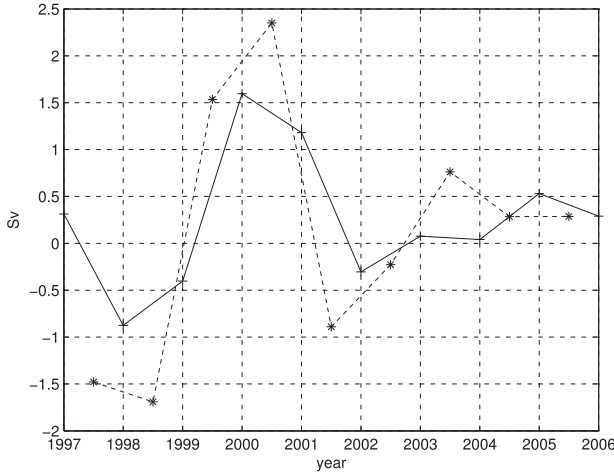


FIG. 5. Year-mean variation of the volume of Ω ($\Delta V/\Delta t$) (dashed line) and sum of the surface formation rate plus exit side flux (solid line). Ordinate is Sv.

a. Potential vorticity in Cartesian coordinates

The evolution equation for PV is

$$\frac{\partial}{\partial t} \rho_0 Q + \nabla \cdot \mathbf{J} = 0, \quad (20)$$

with \mathbf{J} the flux vector of PV. The sum of advective and nonadvective contributions is

$$\mathbf{J} = \rho_0 Q \mathbf{u} + \boldsymbol{\omega} \frac{D\sigma}{Dt} + \mathbf{F} \times \nabla \sigma + \frac{\Phi}{\rho_0} \nabla \rho \times \nabla \sigma, \quad (21)$$

where Φ is the geopotential, ρ the in situ density, and \mathbf{F} the nonconservative force in the momentum equation. After some manipulation of the momentum equation, one can rewrite \mathbf{J} as

$$\mathbf{J} = \boldsymbol{\omega} \frac{\partial \sigma}{\partial t} + \left(\frac{\partial \mathbf{u}}{\partial t} + \nabla B \right) \times \nabla \sigma, \quad (22)$$

where B is the Bernoulli function and

$$B = \frac{1}{\rho_0} \left(P + \rho g z + \rho \frac{u^2}{2} + \rho \frac{v^2}{2} \right), \quad (23)$$

the sum of the pressure, potential, and kinetic energy (e.g., Marshall et al. 2001).

b. PV budget—impermeability theorem

We proceed with a volume integration similar to that discussed in the previous section. Integrated over the control volume Ω , Eq. (20) is

$$\int_{\Omega(t)} \frac{\partial}{\partial t} \rho_0 Q + \int_{\Omega(t)} \nabla \cdot \mathbf{J} = 0. \quad (24)$$

The result, sometimes referred to as the Reynolds transport theorem, is

$$\frac{d}{dt} \int_{\Omega(t)} Q dV = \int_{\Omega(t)} \frac{\partial Q}{\partial t} dV + \int_{\partial\Omega(t)} (\mathbf{u}^s \cdot \mathbf{n}) Q dA, \quad (25)$$

in which \mathbf{n} is the outward-pointing unit normal, and $\mathbf{u}^s = -\mathbf{n}(\partial\sigma/\partial t)/|\nabla\sigma|$ is the normal velocity at a given location of the bounding isopycnal surface.

Using the divergence theorem, we have

$$\frac{d}{dt} \int_{\Omega(t)} \rho_0 Q dV - \int_{\partial\Omega(t)} \rho_0 Q \mathbf{u}^s \cdot \mathbf{n} dA + \int_{\partial\Omega(t)} \mathbf{J} \cdot \mathbf{n} dA = 0. \quad (26)$$

We use the formulation of \mathbf{J} given in Eq. (21) and divide Eq. (21) into components parallel to (denoted by the symbol \parallel) and orthogonal to the isopycnal surface (Marshall and Nurser 1992),

$$\begin{aligned} \mathbf{J} = \rho_0 Q \left(\mathbf{u}_{\parallel} + \frac{\mathbf{u} \cdot \nabla \sigma}{|\nabla \sigma|^2} \nabla \sigma \right) + \frac{D\sigma}{Dt} \left(\boldsymbol{\omega}_{\parallel} + \frac{\boldsymbol{\omega} \cdot \nabla \sigma}{|\nabla \sigma|^2} \nabla \sigma \right) \\ + \mathbf{F} \times \nabla \sigma + \frac{\Phi}{\rho_0} \nabla \rho \times \nabla \sigma. \end{aligned} \quad (27)$$

Using the definition of PV [Eq. (12)], and regrouping the terms parallel to and orthogonal to the isopycnal surface, we have

$$\mathbf{J} = \mathbf{J}_{\parallel} - \rho_0 Q \frac{\partial \sigma / \partial t}{|\nabla \sigma|^2} \nabla \sigma, \quad (28)$$

with \mathbf{J}_{\parallel} the component of \mathbf{J} parallel to an isopycnal surface. We then use the definition of the isopycnal displacement velocity

$$\mathbf{u}_{\sigma\perp} = -\frac{\partial \sigma / \partial t}{|\nabla \sigma|^2} \nabla \sigma, \quad (29)$$

to rewrite Eq. (26) as

$$\begin{aligned} \frac{d}{dt} \int_{\Omega(t)} \rho_0 Q dV - \int_{\partial\Omega(t)} \rho_0 Q (\mathbf{u}^s - \mathbf{u}_{\sigma\perp}) \cdot \mathbf{n} dA \\ + \int_{\partial\Omega(t)} \mathbf{J}_{\parallel} \cdot \mathbf{n} dA = 0. \end{aligned} \quad (30)$$

By our definition of the volume Ω on the two isopycnal surfaces Σ_{σ_1} and Σ_{σ_2} , we have $\mathbf{u}^s = \mathbf{u}_{\sigma\perp}$ and $\mathbf{J}_{\parallel} \cdot \mathbf{n} = 0$. Only the side and the surface contribution are nonzero as per the impenetrability theorem (Haynes and McIntyre 1987),

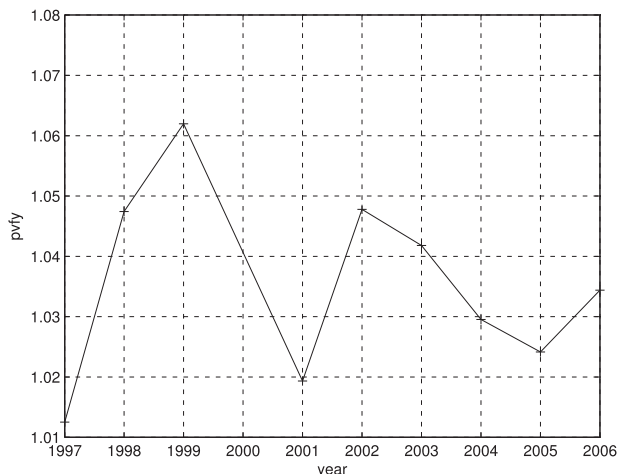


FIG. 6. Ten-year time series of the PV enclosed in Ω . Ordinate is pvfy.

$$\frac{d}{dt} \int_{\Omega(t)} \rho_0 Q dV + \int_{\Sigma_s} \mathbf{J}_{\parallel} \cdot \mathbf{n} dA + \int_{\Sigma_o} J_z dA = 0, \quad (31)$$

with J_z the vertical component of the \mathbf{J} vector. The time average of this last equation returns

$$\overline{\int_{\Sigma_s(t)} \mathbf{J}_{\parallel} \cdot \mathbf{n} dA} + \overline{\int_{\Sigma_o(t)} J_z dA} = 0. \quad (32)$$

This equation states that there is a balance between the mean flux of PV at the surface and the mean flux of PV at the side of our domain.

c. Numerical validation

To examine Eq. (32), we again use a 10-yr time series from the NATL12 run. For the sake of discussion, we introduce a unit for the volume flux of PV: 1 pvf $\equiv 1 \text{ kg m}^{-1} \text{ s}^{-2}$ (which are the units of \mathbf{J} : the flux of PV times an area). In terms of this unit, 1 pvfy corresponds to the quantity of PV given by a flux of 1 pvf sustained during 1 year (a similar interpretation applied to the quantity Svy).

First, we compute the time series of the PV enclosed in the volume Ω . The mean of this time series (shown in Fig. 6) is 1.03 pvfy. The time series is remarkably stable with a standard deviation of these 10 points of 0.01 pvfy (which corresponds to about 1% of the total PV content). Compared to the volume budget, these variations are very small.

The stability of this time series is attributed to the particular choice of control volume Ω . From the definition of PV in Eq. (13), integrating vertically within a layer returns $Q_{\text{int}} = (f + \mathbf{k} \cdot \nabla \times \mathbf{u})(\sigma_2 - \sigma_1)$. Only the relative vorticity content affects the global PV budget;

the thickness of the layer does not appear in the total PV. Again, this reflects that our control volume uses isopycnals as boundaries.

It is also true that the position of the outcrop will affect the global PV-mean content. In fact, during days when the isopycnals outcrop inside \mathcal{C} , the size of the integrated PV decreases accordingly. Also, while the control volume outcrops inside \mathcal{C} , there is a non-zero contribution to the budget from the PV flux at the surface. As soon as the outcrop is completely outside \mathcal{C} , the impermeability theorem argues that the only variation in the integrated PV is due to relative vorticity.

1) SURFACE PV FLUX

The surface PV flux in Eq. (32) is obtained by retaining only the vertical component of Eq. (21) or, equivalently, Eq. (22). We prefer the second formulation since it is easier to compute.

When doing an averaging following an outcrop, we keep only the last term in Eq. (22); namely $\nabla B \times \nabla \sigma$ (see Marshall et al. 2001; D13). Fuller analyses (not shown here) argue that this is an extremely accurate approximation. The conditional (i.e., outcrop following) averaging performed in the domain Ω results in PV extraction at a rate of 0.01 ± 0.02 pvf, which corresponds to less than 1% of the total PV content over a year. Equivalently, this is a PV renewal time scale of 100 yr. This number is consistent with the global variation of the PV from year to year (Fig. 6).

2) INTERIOR PV FLUX

Equation (32) argues the surface flux must be balanced by the lateral PV flux out of Ω . We now check this balance to support our surface computation. As shown in Marshall et al. (2001), time-averaging Eq. (22) equates the mean PV flux to gradients of the Bernoulli in regions where the isopycnal does not outcrop (see also D13), making the mean Bernoulli the streamfunction for the mean PV flux in such areas. Therefore, we can compute the PV flux through the sides of Ω using the mean Bernoulli.

The mean Bernoulli function is plotted for the mode water area (Fig. 7). It is computed as the mean of the vertical integral through the control volume. On this plot, we see two recirculation zones (northeast and northwest, just south of the mean Gulf Stream path). For the rest of the domain, the main pattern is dominated by a northward flux in the center.

In the upper panel of Fig. 7, the value of the Bernoulli function on the contour of the domain is plotted. Numbers in red correspond to the red numbers in the lower panel.

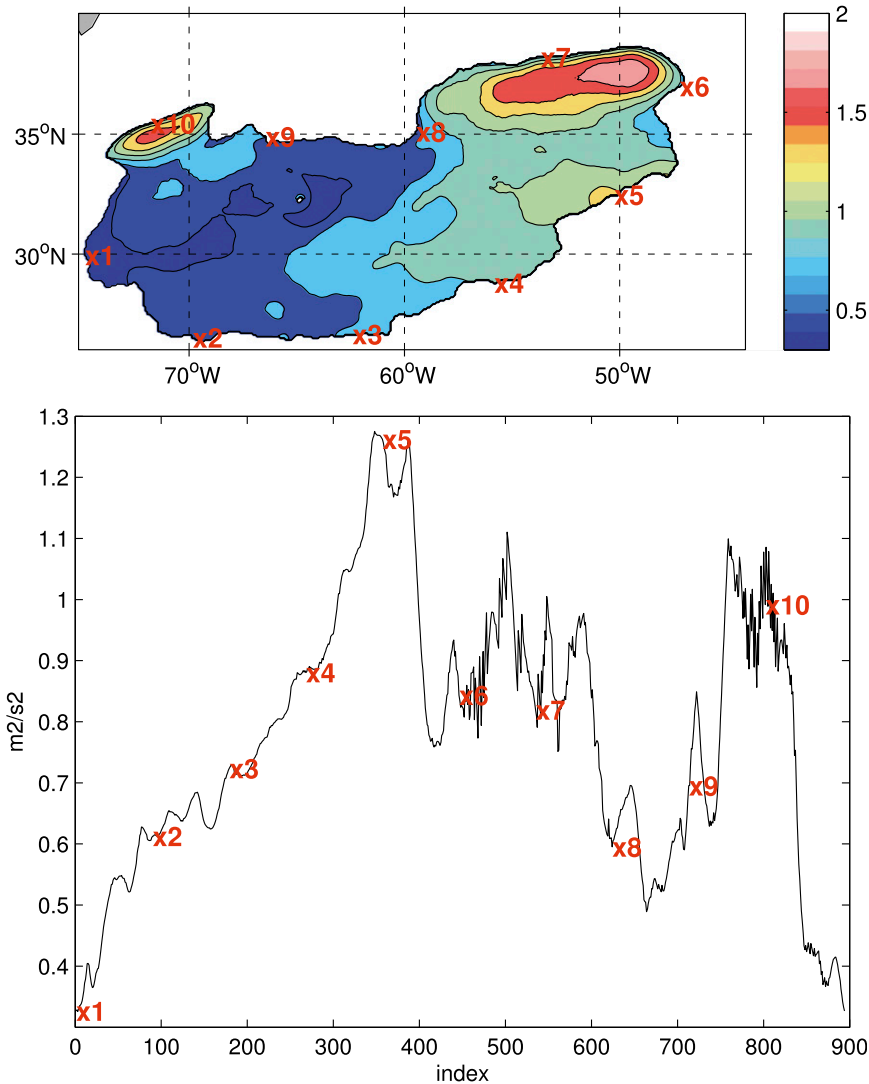


FIG. 7. (top) Mean Bernoulli function in Ω (m^2s^{-2}) and (bottom) value of the Bernoulli function on the contour C . The abscissa is an index along the contour. The red numbers correspond to the locations in the upper plot.

The circulation theorem tells us that the maximum PV extraction is given by the maximum difference of Bernoulli function between two points of the contour. This maximum difference is obtained between points 1 and 5, located on the west and east sides of the domain, respectively. This PV extraction can occur only during winter when the outcrop intersects the contour. To give an upper limit of the PV extraction, we suppose that the outcrop is between points 1 and 5 during 3 months of the year (which corresponds to only $1/4$ of the total). The maximum PV flux is estimated as

$$\Delta\sigma \times \Delta B \times \text{time fraction} = 0.2 \times 1 \times 0.25 = 0.05 \text{ pvf.} \tag{33}$$

This number confirms that only a very small fraction of the total PV can be extracted during a year by surface processes.

We can improve this estimate of the PV flux by using the real position of the outcrop and the instantaneous advective PV flux. The computation returns a value of 0.02 ± 0.03 pvf, which corresponds to a 50-yr PV renewal and is in good agreement with the surface flux obtained using the vertical component of the \mathbf{J} vector.

5. Linking the two budgets

The numbers obtained in the PV budget and mass budget are quite different (a few percent in the first case

and 25% in the second case). This apparent discrepancy is addressed in this section in which we link the two budgets. This is done using a mean-eddy decomposition of the PV budget.

a. Mean-eddy decomposition

There are several ways to write the first term of Eq. (32). Since one of our interests is to link this budget with the Walin computation of the previous section, we can use a thickness-weighted mean decomposition.

The PV fluxes parallel to isopycnals at the domain boundary $\partial\Omega$ can be decomposed into advective and nonadvective parts (denoted by \mathbf{N})

$$\mathbf{J}_{\parallel} \cdot \mathbf{n} = \rho_0 Q \mathbf{u} \cdot \mathbf{n} + \mathbf{N} \cdot \mathbf{n}. \quad (34)$$

The first integral in Eq. (32) can thus be written

$$\begin{aligned} \int_{\Sigma_s} \mathbf{J}_{\parallel} \cdot \mathbf{n} dA &= \int_C \int_{z_1}^{z_2} \rho_0 Q \mathbf{u} \cdot \mathbf{n} dz dl + \int_{\Sigma_s} \mathbf{N} \cdot \mathbf{n} dA \quad (35) \\ &= \int_C \int_{\sigma_1}^{\sigma_2} z_{\sigma} \rho_0 Q \mathbf{u} \cdot \mathbf{n} d\sigma dl + \int_{\Sigma_s} \mathbf{N} \cdot \mathbf{n} dA. \quad (36) \end{aligned}$$

When time averaging this equation, the time averaging can slide into the spatial integral by replacing Σ_s with \mathcal{C} and multiplying \mathbf{N} by a ‘‘tophat’’ function that takes the value 1 if the surface density lies within our target range. We denote this operation as conditional averaging and symbolize it by $\overline{\quad}^c$.

We can then decompose the PV flux into mean and eddy components (thickness weighted)

$$\begin{aligned} \int_{\Sigma_s} \overline{\mathbf{J}_{\parallel}}^c \cdot \mathbf{n} dA &= \hat{Q} \int_C \int_{\sigma_1}^{\sigma_2} \overline{\mathbf{u} z_{\sigma}}^c \cdot \mathbf{n} d\sigma dl \\ &+ \int_C \int_{\sigma_1}^{\sigma_2} \overline{\mathbf{u}'' Q'' z_{\sigma}}^c \cdot \mathbf{n} d\sigma dl \\ &+ \int_{\Sigma_s} \overline{\mathbf{N}}^c \cdot \mathbf{n} dA. \quad (37) \end{aligned}$$

In this last equation, we pull \hat{Q} out of the integral because it is constant on \mathcal{C} . This is precisely why we choose this definition of the control volume: it reveals the link between the mass budget and the PV budget as we now recognize the quantity \hat{Q} multiplies as the net mass flux divergence within \mathcal{C} , which can be computed from the Walin analysis. Furthermore, this decomposition reveals the different actions of the mean flow and the eddies. The third term on the rhs of Eq. (37) is by far the smallest and is neglected from here on. We evaluate both remaining terms numerically.

b. Mean flow

The contribution of the mean flow to the PV budget is given by the first term on the rhs of Eq. (37), formally

$$\hat{Q} \int_{\Sigma_s} \overline{\mathbf{u} z_{\sigma}}^c \cdot \mathbf{n} d\sigma dl. \quad (38)$$

The value of the integral is known from the volume budget and is 2.5 Sv. This implies that the PV flux through Σ_s owing to the mean flow is 0.25 ± 0.09 pvf. This number is much larger than the total surface flux of PV ($\simeq 0.01$ pvf).

c. Eddies

If 25% of the PV is extracted by the mean flow in one year and yet the total budget is nearly balanced, the eddies must be responsible for bringing PV into the domain at a similar rate. This term is formally written as

$$\int_{\Sigma_s} \overline{\mathbf{u}'' Q'' z_{\sigma}}^c \cdot \mathbf{n} d\sigma dl. \quad (39)$$

A long time series is needed to compute the quantity accurately (Rix and Willebrand 1996; Eden et al. 2007). The evaluation of this quantity on Ω shows that the eddies input PV at a rate of 0.28 ± 0.06 pvf, a number that is consistent with the value of the total budget and the value of the mean flow.

The global structure of the eddy field is in good agreement with the classical downgradient sense of eddy PV flux that is at the heart of much theoretical work (Rhines and Young 1982). In D13, we compare this field with $\kappa \nabla Q$ (not shown here). The two fields appear to have the same structure, and we estimate κ between 1000 and 10 000 $\text{m}^2 \text{s}^{-1}$. That the eddies act downgradient also explains the lack of structure in the field inside the domain. This domain is a broad pool of low PV water and hence ∇Q approximately vanishes.

This downgradient mixing property also explains why the eddies are so active in this isopycnal layer: the presence of the mode water intensifies the gradient of PV around the edges of the mode water domain. The role of the eddies in different layers remains to be studied.

6. Comparisons with theory

The previous diagnosis emphasizes the role of eddies in maintaining the spatial distribution of the time-mean PV minimum identified as EDW. In this sense, it supports the basic theory in Dewar (1986). The surprise in the diagnosis is the relative insensitivity of the PV balance to the direct forcing of PV by the atmosphere,

replacing it instead by the Walin water-mass formation mechanism as the primary EDW forcing function. It is interesting to revisit the quasigeostrophic framework of Dewar to illustrate where in the theory this effect enters.

Following classical quasigeostrophic reasoning, such as that in Pedlosky (1987), one arrives at the vorticity equation

$$\frac{\partial}{\partial t}(\zeta + \beta y) + \nabla \cdot [\mathbf{u}_0(\zeta + \beta y) + f_0 \mathbf{u}_1] = 0, \quad (40)$$

where subscripts 0 and 1 denote the usual expansion in the Rossby number. This equation has the advantage of immediately being in conservative form, as is the equation for the Ertel potential vorticity in Eq. (20). To the generalized flux inside the divergence in Eq. (40), we add and subtract the quantity

$$\mathbf{u}_0 \frac{f_0 h_0}{H}, \quad (41)$$

and time average, turning Eq. (40) into

$$\nabla \cdot \left(\overline{\mathbf{u}_0 q} + \overline{\mathbf{u}'_0 q'} + \frac{f_0}{H} \overline{\mathbf{u}_0 h_0} + \overline{f_0 \mathbf{u}_1} \right) = 0, \quad (42)$$

with H the mean thickness of the layer and h_0 the thickness anomaly. In Eq. (42), the quantity q is

$$q = \zeta + \beta y - \frac{f_0}{H} h_0, \quad (43)$$

and is recognized as the usual quasigeostrophic PV. If Eq. (42) is integrated over an area bounded by a line of constant \bar{q} , the first contribution in (42) vanishes.

The layer mass equation can be written

$$\frac{\partial h_0}{\partial t} + \nabla \cdot (\mathbf{u}_0 h_0) + H \nabla \cdot \mathbf{u}_1 = -S, \quad (44)$$

where S parameterizes the water-mass conversion in a QG setting. If Eq. (44) is time averaged and integrated over the same area as Eq. (42), one obtains

$$\int \overline{(\mathbf{u}_0 h_0 + H \mathbf{u}_1)} \cdot \mathbf{n} \, dl = - \iint S \, dA. \quad (45)$$

The mass equation implies the mass flux out of any region to $O(\text{Rossby number})$ must balance the net diabatic injection across the layer interface inside that region. Note that this may be substituted into the area integrated PV equation to yield

$$\int \overline{\mathbf{u}' q'} \cdot \mathbf{n} \, dl = \frac{f_0}{H} \iint S \, dA. \quad (46)$$

The quantity standing in front of the diabatic formation, f_0/H , is recognized as the leading-order mean state

potential vorticity of a quasigeostrophic layer, so the right-hand side represents the potential vorticity cost of a Walin mass flux out of a closed domain. Equation (46) is the quasigeostrophic form of the balance inferred in this paper. It is also identical to the fundamental equation of Dewar (1986) and connects the results herein to that mode water explanation.

We also learn from this analysis how to generalize the mode water PV equation beyond the quasigeostrophic framework inherent in Eq. (6). The basic PV mode water balance that emerges is

$$\nabla \cdot \overline{z_\sigma \mathbf{u} Q} = 0 \quad (47)$$

because of the higher order, weak character of the external PV forcing. Integrating the above over C and separating it into its constituents leads to

$$\hat{Q} \iint S \, dA = \int \overline{\mathbf{u}'' q'' z_\sigma} \cdot \mathbf{n} \, dl. \quad (48)$$

The averaged PV flux must be into the domain to balance the Walin formation. Assuming the divergent part of the eddy PV flux can be parameterized as downgradient, the above becomes

$$\hat{Q} \iint S \, dA = -\kappa \int \overline{z_\sigma \nabla \hat{Q}} \cdot \mathbf{n} \, dl. \quad (49)$$

We expect that, in the time mean, the flow on density surfaces should be geostrophic to leading order

$$-f \bar{u} = -\overline{M}_y, \quad (50)$$

$$f \bar{v} = -\overline{M}_x, \quad (51)$$

where M is the Montgomery potential

$$M = \frac{p}{\rho_0} + gz. \quad (52)$$

The mean mass budget on an isopycnal is

$$\nabla \cdot (\overline{\mathbf{u} z_\sigma} + \overline{u' z_\sigma'}) = -S. \quad (53)$$

If the divergent component of the mass flux is presumed to be due to the eddies, then the above reduces to the nondivergence of the Reynolds mean mass flux

$$\nabla \cdot \overline{\mathbf{u} z_\sigma} = 0. \quad (54)$$

Employing geostrophy [the contribution due to the relative vorticity in Eq. (14) is negligible] returns the result, $J(\hat{Q}, \overline{M}) = 0$, or

$$\hat{Q} = \hat{Q}(\overline{M}). \quad (55)$$

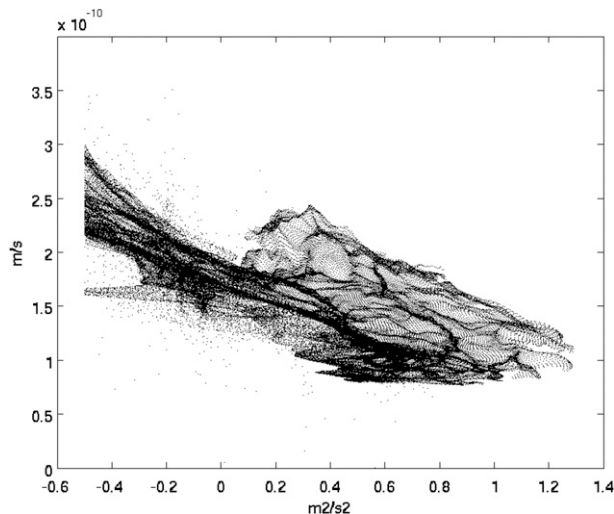


FIG. 8. Scatterplot of \hat{Q} ($\text{m}^{-1}\text{s}^{-1}$) vs \bar{B} ($\text{m}^{-2}\text{s}^{-2}$) restricted to the subtropical gyre ($\bar{B} > -0.5$).

Allowing for some scatter, support for Eq. (55) is shown in Fig. 8 where climatological PV is plotted against the mean Bernoulli function (mean Bernoulli and mean Montgomery functions are essentially indistinguishable). The correlation coefficient between these two variables is 0.8. Note that strong connections exist between these two variables consistent with Eq. (55).

Using Eq. (55) in Eq. (49) then returns the generalized mode water PV equation:

$$\frac{\partial \hat{Q}}{\partial \bar{M}} = \left(\frac{-\iint S dA}{\kappa \int z_{\sigma} \nabla \bar{M} \cdot \mathbf{n} dl} \right) \hat{Q}. \quad (56)$$

Note that the nonconstant coefficient of this equation is negative for areas receiving a nonzero Walin forcing in an anticyclonic circulation like that in the North Atlantic subtropical gyre. Thus, climatological PV for such zones is expected to decrease in the direction of high pressures, which naturally occur at the center of anticyclones. Once the enclosed areas no longer encapsulate Walin input, PV is predicted to be constant. The implied PV structure is consistent with the existence of mode waters and is in qualitative agreement with the numerical results. Much of this is essentially like the quasigeostrophic balance; the distinction that occurs is in the appearance of the climatological PV on the rhs of Eq. (56).

7. Summary and conclusions

a. Summary

We computed the mass budget and the PV budget of the core of the subtropical Atlantic mode water. The

mass budget, which is linked to the surface buoyancy flux (Walin 1982), is computed numerically using a 10-yr time series of a numerical model (Treguier 2008). We show that the surface heat fluxes are responsible for adding 2.5 Svy in the core of the mode water. This addition occurs only in winter when the mode water is in direct contact with the atmosphere. This newly formed water is evacuated through the side at the same rate.

The second part of this paper examines a PV budget of the mode water. We show that the global PV output at the surface is a small fraction of the total PV content (a few percent). This surface output is balanced on the side by the same amount of input of PV. When we continue dissecting this budget by separating the mean contribution from the eddy contribution, we find that these two components are fairly large and balance each other. We explain this nontrivial result with the aid of the volume budget. Since the mean flow has to be in the direction of mass export through the sides of the domain (in order to balance the surface creation), this outward flow will export PV at the same rate. On the other hand, eddies act to counterbalance this PV flux and efficiently bring PV into this region.

Linking these two budgets provides a better vision of mode water dynamics. It is clear that the low PV water is the result of surface water-mass formation and not PV extraction. Once this low PV water is created, it is entrained by the mean flow. At the same time eddies tend to mix this low PV water with the higher PV surrounding water.

b. Implications for future work

Equation (55) makes a series of predictions for isopycnals above and below the mode water. For deeper layers, barely in contact with the atmosphere, we would expect small (if any) water-mass creation; at the same time the homogenized pool of PV for this layer should encompass more of the circulation. If there is no water-mass creation, there should be no mean mass flux out of any closed circulation contours, and hence no PV entrainment required by the mean flow. This implies a vanishing PV/mass transport by the eddies. If we recall that the eddies act as $\kappa \nabla Q$, it is consistent to expect very little action by the eddies in a layer of homogenized PV.

For shallower layers, the role of Walin ventilation should grow and even change sign. The above arguments make predictions about the structure of PV on these layers, but the extent to which these are accurate remains unclear. Examination of the PV budgets for layers aside from the mode water is a topic for further exploration. A related open question is the role of the divergent and rotational part of both the mean flow and the eddies (Eden et al. 2007). How do these two contributions evolve from one layer to the next?

The question of the low frequency variability of mode water also remains open. In the time series shown in this paper, we noted sizable variations from year to year in terms of formation, dissipation, and storage. It would be an interesting question to relate these low frequency variations to the large-scale circulation and the impact on the atmospheric dynamics.

Finally, we saw in D13 that the structure of the Bernoulli function changes with depth owing to an increasing contribution of the thermobaric term. The mode water is located precisely at the level at which the Bernoulli circulation is the weakest. This last point requires more investigation to understand the role of thermobaricity in mode water dynamics.

Acknowledgments. We are grateful to A.-M. Treguier and J.-M. Molines for providing the model data and helpful discussions. We would also like to thank K. Fearon for her inputs on the final version of the manuscript. The work reported here was sponsored by NSF Grant OCE-0960500. The comments of two anonymous reviewers are gratefully acknowledged.

REFERENCES

- Czaja, A., and U. Hausmann, 2009: Observations of entry and exit of potential vorticity at the sea surface. *J. Phys. Oceanogr.*, **39**, 2280–2294.
- D'Asaro, E., C. Lee, L. Rainville, R. Harcourt, and L. Thomas, 2011: Enhanced turbulence and energy dissipation at ocean fronts. *Science*, **332**, 318–322, doi:10.1126/science.1201515.
- Deremble, B., and W. K. Dewar, 2012: First-order scaling law for potential vorticity extraction due to wind. *J. Phys. Oceanogr.*, **42**, 1303–1312.
- , N. Wienders, and W. K. Dewar, 2013: Potential vorticity budgets in the North Atlantic Ocean. *J. Phys. Oceanogr.*, in press.
- Dewar, W. K., 1986: On the potential vorticity structure of weakly ventilated isopycnals: A theory of subtropical mode water maintenance. *J. Phys. Oceanogr.*, **16**, 1204–1216.
- , R. M. Samelson, and G. K. Vallis, 2005: The ventilated pool: A model of subtropical mode water. *J. Phys. Oceanogr.*, **35**, 137–150.
- Eden, C., R. J. Greatbatch, and J. Willebrand, 2007: A diagnosis of thickness fluxes in an eddy-resolving model. *J. Phys. Oceanogr.*, **37**, 727–742.
- Forget, G., G. Maze, M. Buckley, and J. Marshall, 2011: Estimated seasonal cycle of North Atlantic Eighteen Degree Water volume. *J. Phys. Oceanogr.*, **41**, 269–286.
- Gent, P. R., and J. C. McWilliams, 1990: Isopycnal mixing in ocean circulation models. *J. Phys. Oceanogr.*, **20**, 150–160.
- Hanawa, K., and L. D. Talley, 2001: Mode waters. *Ocean Circulation and Climate: Observing and Modelling the Global Ocean*, G. Siedler et al., Eds., International Geophysics Series, Vol. 77, Academic Press, 373–386.
- Haynes, P. H., and M. E. McIntyre, 1987: On the evolution of vorticity and potential vorticity in the presence of diabatic heating and frictional or other forces. *J. Atmos. Sci.*, **44**, 828–841.
- Marshall, D. P., 2000: Vertical fluxes of potential vorticity and the structure of the thermocline. *J. Phys. Oceanogr.*, **30**, 3102–3112.
- Marshall, J. C., and A. J. G. Nurser, 1992: Fluid dynamics of oceanic thermocline ventilation. *J. Phys. Oceanogr.*, **22**, 583–595.
- , D. Jamous, and J. Nilsson, 1999: Reconciling thermodynamic and dynamic methods of computation of water-mass transformation rates. *Deep-Sea Res.*, **46**, 545–572, doi:10.1016/S0967-0637(98)00082-X.
- , —, and —, 2001: Entry, flux, and exit of potential vorticity in ocean circulation. *J. Phys. Oceanogr.*, **31**, 777–789.
- Maze, G., and J. Marshall, 2011: Diagnosing the observed seasonal cycle of Atlantic subtropical mode water using potential vorticity and its attendant theorems. *J. Phys. Oceanogr.*, **41**, 1986–1999.
- , G. Forget, M. Buckley, J. Marshall, and I. Cerovecki, 2009: Using transformation and formation maps to study the role of air–sea heat fluxes in North Atlantic Eighteen Degree Water formation. *J. Phys. Oceanogr.*, **39**, 1818–1835.
- , J. Deshayes, J. Marshall, A.-M. Treguier, A. Chronis, and L. Vollmer, 2013: Surface vertical PV fluxes and subtropical mode water formation in an eddy-resolving numerical simulation. *Deep-Sea Res.*, **91**, 128–138.
- Nurser, A. J. G., R. Marsh, and R. G. Williams, 1999: Diagnosing water mass formation from air–sea fluxes and surface mixing. *J. Phys. Oceanogr.*, **29**, 1468–1487.
- Olsina, O., N. Wienders, and W. K. Dewar, 2013: An estimate of the climatology and variability of Eighteen Degree Water potential vorticity forcing. *Deep-Sea Res.*, **91**, 84–95, doi:10.1016/j.dsr.2.2013.02.018.
- Pedlosky, J., 1987: *Geophysical Fluid Dynamics*. 2nd ed. Springer-Verlag, 636 pp.
- Peterson, K., and R. Greatbatch, 2001: Vorticity fluxes in shallow water ocean models. *Atmos.–Ocean*, **39**, 1–14.
- Rhines, P. B., and W. R. Young, 1982: Homogenization of potential vorticity in planetary gyres. *J. Fluid Mech.*, **122**, 347–367, doi:10.1017/S0022112082002250.
- Rix, N. H., and J. Willebrand, 1996: Parameterization of mesoscale eddies as inferred from a high-resolution circulation model. *J. Phys. Oceanogr.*, **26**, 2281–2285.
- Speer, K., and E. Tziperman, 1992: Rates of water mass formation in the North Atlantic Ocean. *J. Phys. Oceanogr.*, **22**, 93–104.
- The Climode Group, 2009: The Climode field campaign: Observing the cycle of convection and restratification over the Gulf Stream. *Bull. Amer. Meteor. Soc.*, **90**, 1337–1350.
- Thomas, L. N., 2005: Destruction of potential vorticity by winds. *J. Phys. Oceanogr.*, **35**, 2457–2466.
- Treguier, A. M., 2008: DRAKKAR NATL12 model configuration for a 27-year simulation of the North Atlantic Ocean. DRAKKAR Tech. Rep. lpo-2008-05, 15 pp. [Available online at <http://www.drakkar-ocean.eu/publications/report/natl12-2008.pdf>.]
- , I. M. Held, and V. D. Larichev, 1997: Parameterization of quasigeostrophic eddies in primitive equation ocean models. *J. Phys. Oceanogr.*, **27**, 567–580.
- , J. Deshayes, C. Lique, R. Dussin, and J. M. Molines, 2012: Eddy contributions to the meridional transport of salt in the North Atlantic. *J. Geophys. Res.*, **117**, C05010, doi:10.1029/2012JC007927.
- Walín, G., 1982: On the relation between sea-surface heat flow and thermal circulation in the ocean. *Tellus*, **34**, 187–195.
- Warren, B. A., 1972: Insensitivity of subtropical mode water characteristics to meteorological fluctuations. *Deep-Sea Res.*, **19**, 1–19, doi:10.1016/0011-7471(72)90069-1.
- Worthington, L., 1958: The 18° Water in the Sargasso Sea. *Deep-Sea Res.*, **5**, 297–305, doi:10.1016/0146-6313(58)90026-1.